Covalently linked dengue virus envelope glycoprotein dimers reduce exposure of the immunodominant fusion loop epitope

Alexander Rouvinski[1,2*¶], Wanwisa Dejnirattisai[3*], Pablo Guardado-Calvo[1,2*], Marie-Christine Vaney[1,2], Arvind Sharma[1,2], Stéphane Duquerroy[1,2,4], Piyada Supasa[3], Wiyada Wongwiwat[3], Ahmed Haouz[5], Giovanna Barba-Spaeth[1,2], Juthathip Mongkolsapaya[3,6§], Félix A. Rey[1,2§] and Gavin R. Screaton[3§]

[1]Institut Pasteur, Département de Virologie, Unité de Virologie Structurale, 75724 Paris Cedex 15, France.

[2]CNRS UMR 3569 Virologie, 75724 Paris Cedex 15, France

[3]Division of Immunology and Inflammation, Department of Medicine, Hammersmith Hospital Campus, Imperial College London, w12 0NN London, UK

[4]Université Paris-Sud, Faculté des Sciences, 91405 Orsay, France

[5]Institut Pasteur, Protéopôle, CNRS UMR 3528, 75724 Paris Cedex 15, France

[6]Dengue Haemorrhagic Fever Research Unit, Office for Research and Development, Siriraj Hospital, Mahidol University, Bangkok 10700, Thailand

[*]These authors contributed equally.

Present address: Hebrew University of Jerusalem, School of Medicine, Department of Microbiology and Molecular Genetics, Israel.

Corresponding authors: JM (j.mongkolsapaya@imperial.ac.uk); FAR (felix.rey@pasteur.fr); GRS (g.screaton@imperial.ac.uk).

Abstract

A problem in the search for an efficient vaccine against dengue virus is the immunodominance of the fusion loop epitope (FLE), a segment of the envelope protein E that is buried at the interface of the E dimers coating mature viral particles. Anti-FLE antibodies are broadly cross-reactive but poorly neutralizing, displaying a strong infection enhancing potential. FLE exposure takes place via dynamic "breathing" of E dimers at the virion surface. In contrast, antibodies targeting the E dimer epitope (EDE), readily exposed at the E dimer interface over the region of the conserved fusion loop, are very potent and broadly neutralizing. We have engineered E dimers locked by inter-subunit disulphide bonds, and show here by X-ray crystallography and by binding to a panel of human antibodies that these engineered dimers do not expose the FLE while retaining the EDE exposure. These locked dimers are strong immunogen candidates for a next-generation vaccine.

Introduction

Certain members of the Flavivirus genus are the most important arthropod borne viral pathogens of humans, causing increasingly serious disease outbreaks. The flaviviral disease that imposes the highest toll on society is dengue, which is caused by four different viruses termed serotypes DENV1-4, differing by 30-35% in amino acid sequence of their envelope proteins[1]. It is estimated that the annual global incidence is 390 million cases, of which 96 million are clinically apparent, with around 25 thousand deaths[2]. Several factors drive the pandemic, including globalization, the spread of the *Aedes* mosquito vector around the world, inadequately planned urbanization, and absence until recently of a licensed vaccine or anti-DENV therapeutics[3-5]. Zika virus (ZIKV) is also transmitted by *Aedes* mosquitos, and among the flaviviruses, its envelope protein is closest in amino acid sequence (about 56% identity) to that of the DENVs than to other flaviviruses[6].

The hallmark of severe DENV infection is increased capillary permeability, causing plasma leakage and bleeding, leading to haemodynamic compromise and DENV shock syndrome[1]. Untreated, severe disease can lead to a mortality of up to 20%, but with expert management, primarily fluid replacement, it can be reduced to below 1%. DENV has caused explosive epidemics, putting huge stress on healthcare systems in endemic countries. Although several

DENV control strategies are being evaluated, it is generally agreed that an effective vaccine available to all age groups is required to make serious inroads into the burden of disease[1,5].

Infection with one serotype of DENV results in the generation of lifelong immunity to reinfection with that serotype but not to the others[1]. As all four DENV serotypes frequently co-circulate, or cyclically replace each other, multiple infections are the norm in endemic countries. Well-controlled epidemiological studies demonstrate that most severe DENV infections occur in individuals who are experiencing a secondary or sequential DENV infection[7].

The hypothesis of antibody dependent enhancement (ADE) posits that pre-existing heterologous antibodies generated during a primary infection may not efficiently neutralize a secondarily encountered virus[8]. Instead, the virus may be opsonized and targeted for uptake into Fc-receptor bearing cells such as monocytes and macrophages, which are important sites of DENV replication *in vivo*, and therefore lead to an increase in viral production.

There have now been a number of descriptions of human monoclonal antibodies in DENV infection[9-16]. The immunodominant epitope to DENV appears to be the FLE, a linear epitope spanning the fusion loop, which is highly conserved in flaviviruses. Anti-FLE mAbs are frequently cross-reactive across all DENV serotypes and also across flaviviruses[9,12,17]. Because the FLE is sub-optimally presented by mature flaviviruses, anti-FLE mAb often show poor neutralization but potently induce ADE[9,12,17-19]. PrM-specific antibodies are also a major component of the memory B cell response to DENV; these antibodies show poor neutralization (maximum 30-50%) even at high concentration[20].

We have recently described the cloning of a large panel of anti-E mAbs from DENV infected patients[12]. One third of the antibodies generated recognize a conformational, quaternary epitope and bind poorly to the recombinant E ectodomain (termed sE), which is mainly monomeric in solution. Many of these antibodies showed broad and potent neutralization of all four DENV serotypes, being amongst the most potent described to date. Structural characterization has shown that these mAbs bind to the E dimers at the virion surface, to a site that we termed the E-dimer epitope (EDE). In addition, we have recently discovered that the epitope recognized by some anti-EDE antibodies is also conserved in the ZIKV E-dimer, leading to equally potent neutralization, making the EDE also a potential target for ZIKV vaccines[6,21]. The observation that broadly neutralizing antibodies can be produced during DENV infection suggests that using

subunit vaccines targeting the EDE is an alternative route for vaccines. We describe here covalently linked dengue envelope dimers that can be produced in the absence of prM and which also reduce exposure of the immunodominant FLE aiming to suppress the generation of unwanted yet ADE promoting antibody responses.

Results

Anti-EDE mAbs can stabilize the E-dimer

Binding of anti-EDE antibodies to sE requires the presence of head-to tail-dimers that form only at high concentrations in solution - such as the concentrations used for crystallization, which mimic the very high effective E protein concentration at the surface of virus particles. This is exemplified when monomeric recombinant sE protein is plate bound in ELISA assays where antibodies such as those to FLE bind well whilst those reacting to the EDE do not (Fig. 1a). But when the ELISA is performed in reverse (capture ELISA) and anti-EDE mAb is bound to the plate it is able to capture sE protein, by shifting the monomer-dimer equilibrium (Fig. 1b), which cannot be achieved when the monomeric form is immobilized.

Anti-EDE antibodies can be divided into two subclasses depending on their sensitivity to the presence of the N-linked glycan at position 153, which is required for anti-EDE2 mAb binding but not required for the anti-EDE1 mAbs binding[12]. In the capture ELISA assays described above, EDE1 C8 and EDE2 A11 antibodies were able to drive dimer formation at lower concentrations of E protein compared to EDE1 C10 and EDE2 B7, which probably represents a higher affinity of interaction with the recombinant sE-dimer (Fig. 1b). The ability of anti-EDE mAb to drive dimer formation is further exemplified by size exclusion chromatography together with multi-angle static light scattering (MALS) where EDE1 C8 or EDE2 A11 Fabs assemble sE into a sE dimer resulting in the formation of sE/Fab heterotetramer (sE dimer with two bound Fab molecules) (Fig. 1c).

FLE and EDE mAbs compete to bind DENV particles

The X-ray structures of both anti-EDE1 and anti-EDE2 mAbs bound to DENV2 sE showed that they bind at the E dimer interface, at a site where the fusion loop - which is present at the tip of domain II - interacts with domains I and III from the opposite E subunit in the dimer. The EDE

epitope thus spans residues from all 3 domains of E, including the fusion loop but in a conformation such that the non-polar Trp101 and Leu107 side chains are buried at the interface with domain III[22]. In contrast, the FLE antibodies only require residues at the tip of domain II for binding, and specifically recognize the side chains of the fusion loop residues that are buried in the E dimer[23,24]. The anti-EDE and anti-FLE mAbs thus bind when these side chains are buried or exposed, respectively. It is therefore important to understand the extent to which binding of these two classes of antibodies compete with each other for binding DENV particles.

We therefore devised a competition ELISA whereby DENV was captured on ELISA plates and the binding of biotinylated anti-EDE or anti-FLE mAbs assessed in the presence of non-biotinylated mAb competitor (Fig. 2a). In a first series of experiments we fixed the concentration of biotinylated antibody at 1 μg/ml and added an increasing concentration of non-biotinylated antibody. These assays were performed on two different virus preparations, DENV2 produced either in the mosquito cell line C6/36 or in primary human myeloid derived dendritic cells (DC). C6/36 produced viruses have a higher content of uncleaved prM compared to DENV produced in DC (Fig. S1)[12,20]. This difference in prM leads to higher binding and neutralization of C6/36 DENV than DC-DENV by anti-FLE mAb[12]. The neutralization of DC-DENV by anti-FLE mAb is however incomplete with a plateau at around 80% neutralization[12]. In contrast to anti-FLE mAb, anti-EDE mAb are able to bind and fully neutralize DENV produced in both C6/36 cells and DC[12].

Using C6/36 cell derived DENV particles, the anti-FLE mAbs were the most effective competitors for binding to virions and were able to prevent binding of anti-EDE mAbs at high concentrations, whereas anti-EDE mAb as expected, could compete with themselves for binding, but not with anti-FLE mAb (Fig. 2b). When tested on low prM containing DC-DENV, anti-FLE mAb was less effective competitor for anti-EDE binding and anti-EDE mAbs were able to compete off anti-FLE binding (Fig. 2c).

In a second series of experiments we preincubated virions with biotinylated or non-biotinylated anti-FLE or anti-EDE mAbs and then looked for the ability of competitor antibody to displace bound antibody over a time course of incubation. These experiments demonstrate that once bound to DENV the interaction with both anti-FLE and anti-EDE mAbs was very stable and could not be displaced (Fig. S2b-d).

Stabilisation of the E-dimer

We used a structure-based approach to identify pairs of residues at the dimer interface located such that their replacement by cysteine could potentially lead to formation of inter-subunit disulphide bonds and improve sE-dimer stability. We analysed the crystal structure of the DENV2 sE dimer (DENV2 sE in complex with EDE2 B7 Fab, PDB accession code 4UT6, [22]) with the MODIP server (http://caps.ncbs.res.in/iws/modip.html)[25], which identified four pairs of amino acids facing each other across the dimer interface with C_β-C_β distances under 4.5 Å. These were residues S255, A259, F108/T315 and L107/A313. S255 and A259 lie by the molecular 2-fold axis, such that they face themselves in the dimer, and therefore only one mutation to cysteine is required to form a disulphide bond. The other residues are away from the molecular 2-fold axis, at the interface between the fusion loop (which spans residues 98-110) and domain III, and require two mutations to cysteine and thus form two inter-monomer disulphide bonds. The MODIP server ranks the pairs from A to D depending on the adequacy of their geometry to make a disulphide bond, where A is the highest score (meaning a high probability of forming a disulphide bond in the analysed static PDB model) and D the poorest. The location of these residues in the structure of the DENV2 sE dimer, along with the respective MODIP scores, is indicated in Fig. 3a. None of the predicted disulphide had the highest score, indicating a non-optimal geometry. Nevertheless, as the DENV E protein has been shown to be flexible and has several hinge angles, it is likely that its polypeptide chain can adjust to the required geometry to make some of the disulphide bonds.

Production of these four cysteine mutants (two single and two double mutants) in *Drosophila* S2 cells showed that the best yields in disulphide linked sE dimers resulted from the A259C construct followed by the double mutant L107C/A313C (Fig 3b), suggesting that the chain can adjust the geometry in these two cases, but not in the other two mutants. Although these mutants produced also a fraction of monomer and also of high-molecular weight aggregates, they resulted in about 2mg of covalent dimer produced by litre of S2 cell culture, whereas the other two mutants led essentially to only aggregates (Fig. 3b).

Analysis by size exclusion chromatography (SEC) together with multi-angle static light scattering (MALS) of the A259C mutant showed that it eluted in a peak corresponding to a molecular weight of 93 kDalton, as expected for a sE dimer. Under the same conditions, wild type DENV2 sE eluted as two peaks, both corresponding to a monomer (48 kDa MW) according

to the molecular mass measured by MALS (Fig. 3c). The main peak (on the right, in blue) elutes late, indicating interaction with the support, similar to what has been reported previously for other homologous class II viral fusion proteins when manipulated as monomers with the fusion loop exposed[26]. The double mutant L107C/A313C also eluted as a dimer and the peak overlapped with that of A259C (Fig. 3d), as expected. This was also confirmed by SDS-PAGE under reducing and non-reducing conditions (Fig. 3e). We also prepared the mutants equivalent to DENV2 A259C and L107C/A313C for the other DENV serotypes where we were obtaining similar yields, except for DENV1, which resulted only in monomer or aggregates with little dimer formation (Fig. S3), indicating that in the context of the DENV1 E protein sequence, the polypeptide chain cannot adapt to the correct geometry to make the disulphide bond, in contrast to the E protein from the other DENV serotypes.

X-ray structure of the DENV2 sE single and double mutants in complex with EDE2 A11 Fab

In order to confirm that inter-subunit disulphide bond formation did not interfere with the overall conformation of the sE dimer, we carried out structural studies of the DENV2 sE mutants by X-ray crystallography. Because the mutants by themselves did not yield crystals of good enough quality, we tested crystallization in complex with EDE mAb fragments. We obtained crystals of both sE A259C and sE L107C/A313C in complex with Fab EDE2 A11 belonging to the orthorhombic space group $P2_12_12$. The crystals diffracted anisotropically to 3.9 Å along h and l axis and to only 7.2Å (A259C) or 6.2Å (L107C/A313C) along the long b axis. Given the limited resolution and anisotropy of the datasets we carefully selected the resolution cutoffs leading to the statistics shown in Table S1.

Both mutants crystallize with near identical unit cell parameters as the wild-type DENV2 sE-Fab EDE2 A11 complex (PDB accession code 4UTB,[22]), but in a different orthorhombic space group ($P2_12_12$ for the mutants and of $P2_12_12_1$ for the wild type), resulting in a related but non-identical crystal packing. This lack of isomorphism precluded the calculation of an isomorphous difference map (Fo_{Mutant}-$Fo_{WildType}$) with the 4UTB structure. We therefore determined the crystal structures of the mutants by molecular replacement using the 4UTB model as search. The resulting difference electron density maps, after one round of refinement, showed strong positive peaks mapping to the sites where the disulphide bonds were introduced (Fig. S4a).

Refinement of the atomic models of the mutants was done at 3.9 Å resolution avoiding over-fitting the data as much as possible by keeping very tight geometric constraints (Table S1). The results are consistent with the introduction of the disulphide bonds in both sE dimer mutants not inducing a gross rearrangement of the global conformation of the sE dimers, as illustrated in the superpositions displayed in Fig. S5, with a root mean square deviation (RMSD) deviation of 1.11 Å for the A259C mutant and 0.14 Å for the L107C-A313C mutant over 775 superposed Cα atoms. The final refined structures of sE mutants thus have the same overall organization as wild-type sE (Fig. 4), except for the extra disulphide bond located at the 2-fold axis for the sE A259C structure (green arrow in Fig. 4b) and the two extra disulphide bonds connecting the fusion loop with domain III (green arrow in Fig. 4c) for the sE L107C/A313C structure. The resulting electron density maps obtained with the final refined phases (2Fo-Fc map) around the inter-chain disulphide bonds for sE A259C and sE L107C/A313C mutants are displayed in Fig. S4b.

Two disulphide bridges are needed to suppress exposure of the FLE

To verify that EDE epitopes are effectively exposed in our mutant sE dimers, we tested binding to both anti-EDE1 and anti-EDE2 mAbs in a direct ELISA assay (as described in figure 1a) with plate bound recombinant wild type sE protein in comparison to covalently linked sE dimers performed at low E concentration (10ug/ml) (Fig. 5a,5b left panels). Both A259C (Fig. 5a) and L107C/A313C (Fig. 5b) mutants were efficiently recognized by anti-EDE1 and anti-EDE2 antibodies, in contrast to the wild type protein and in line with the crystal structures, showing that the mutant recombinant sE proteins form stable dimers correctly exposing the EDE.

Since the FLE is an immunodominant epitope, it is important to design immunogens that prevent the generation of this suboptimal ADE inducing response. To test whether the stable sE-dimers described above were still capable of exposing the FLE, we tested their reactivity to a panel of FLE reactive human mAbs we have previously described[12].

Binding to the panel of anti-FLE mAbs was tested to sE-dimers and compared to binding to wild type sE (Fig. 5a, 5b right panels). Of note, we found that the single disulphide bonded A259C sE dimer was fully competent to bind the panel of anti-FLE mAbs (Fig. 5a, right panel) whereas binding was largely lost when using the double disulphide bonded L107C/A313C sE dimer (Fig. 5b, right panel). We surmise that A259C mutant, which is linked via a single bond at the centre

of the sE dimer (Fig. 4b), shows a considerable dynamic behaviour, being able to breathe by swivelling around the central disulphide bond and allowing exposure of the FLE. On the other hand, sE dimer L107C/A313C, containing disulphide bonds at each end of the dimer (Fig. 4c), is locked and unable to expose the FLE.

To further confirm this hypothesis, we checked the ability of these two mutants to insert into membranes using a liposome floatation assay. DENV2 WT, A259C and L107C/A313C recombinant proteins were incubated with liposomes under acidic conditions and analysed by western blot after ultracentrifugation on a density gradient (Fig. 5c). Under acidic conditions WT sE inserts into the liposomes and the majority of the protein is found in the top fraction of the gradient (Fig. 5c lanes 1). Mutant A259C was still able to insert into liposomes, as it could be detected in the top fraction of the gradient (Fig. 5c lanes 3) – albeit proportionally less than wild type - whereas no protein co-floated with the liposomes in the L107C/A313C mutant (Fig. 5c lanes 5). These results suggest that in the A259C mutant the fusion loop is partially exposed and is able to insert into membranes as dimer, making weaker interactions than wild-type, which inserts as trimer[27]. This result is in line with the ability of FLE mAbs to bind A259C mutant in the ELISA assay (see above Fig. 5a), and suggests that the two monomers can rotate about the engineered disulphide bond to align parallel to each other for membrane insertion. In the L107C/A313C mutant the fusion loop is not exposed to promote insertion into membranes under acidic conditions, in concordance with reduced FLE exposure shown in Figure 5b. Similar results were obtained for DENV3 and DENV4 (see Fig. 5c).

Discussion

We have shown here that it is possible to engineer covalently locked sE dimers that expose the EDE and are not recognized by most antibodies targeting the FLE. Such stabilized sE dimers can be made in high yields for three out the four DENV serotypes, with the exception of DENV1. We will attempt to express DENV1 dimers in alternative expression systems, however, as the EDE is a cross-reactive epitope, the EDE MAbs efficiently neutralize DENV1 as well as the other serotypes. In the future, priming and boosting by alternating the three DENV serotypes for which the dimers can be obtained should be sufficient to preferentially stimulate B cells producing EDE antibodies, which by definition would also neutralize DENV1. The possibility remains to resurface sE from DENV3 (which is most closely related to DENV1) in the event that

298 a ENV1-like sE molecule with a stable EDE is required, a similar approach has recently been
299 used to graft the DENV3 specific epitope for mAb 5J7 into DENV[28].
300
301 It is now becoming clear that the most potent neutralizing antibodies against DENV target
302 conformationally sensitive epitopes readily exposed at the E dimer surface. Some of these
303 epitopes are contained within a single E subunit, such as the potently DENV4-serotyype
304 specifc mAb-5H2 or the DENV1 specific mAb-1F4, and some are shared by two or more E
305 subunits such as the DENV1 specific mAb-HM14c10 or the DENV2 specific 2D22-mAb,
306 which binds the E-dimer at a position close to the EDE, or the DENV3-specific mAb-5J7,
307 which binds across three adjacent E polypeptides on the virion[13,15,29-31].
308
309 prM-specific antibodies do not bind to fully mature virions – since they do not contain prM -
310 whereas many partially mature particles do not contain a high enough density of prM to allow
311 neutralization but yet may be sufficient to promote ADE[20]. We have speculated that the
312 inefficient cleavage of prM may be an immune evasion/enhancement strategy (indeed, the furin
313 cleavage sequence is suboptimal in DENV prM), leading to the generation of poorly neutralizing
314 antibodies directed to prM. The high frequency, low potency and high ADE potential of
315 antibodies directed to prM has implications for vaccine design; all attenuated vaccines constructs
316 encode prM, although the precise prM content of the virus particles in these vaccines has not
317 been reported. The ideal vaccine would focus responses to E while the prM component of the
318 response be minimized if the potential for ADE in vaccines is to be reduced. The stabilized sE-
319 dimers described here are devoid of prM and will therefore not induce this response.
320
321 Compared to other flaviviruses such as ZIKV, DENV seems to display a higher dynamic
322 behaviour, which combined with incomplete furin maturation allows for exposure of the FLE in
323 particles circulating at neutral pH[32-37]. It is highly likely that the dynamic behaviour of DENV
324 particles may underpin why the FLE is such a dominant epitope in DENV and consequently why
325 it is difficult to produce effective DENV vaccines. Our demonstration that engineering inter-
326 subunit disulphide bonds that do not alter the structure of the E dimer (Fig. 4) and are not
327 recognized by anti-FLE MAbs (Fig. 5) is an important step toward avoiding elicitation of
328 antibodies targeting the FLE. We propose that future vaccines minimizing the anti-FLE response
329 should be pursued as immunogens. The double disulphide bonded DENV2 L107C/A313C dimer
330 described here, where the dimer is effectively locked and does not expose the FLE, is a strong
331 candidate to constitute the basis for such a vaccine. Testing the ability of DENV stabilized dimers to

elicit an anti-EDE response may be complicated as murine antibody responses differ considerably from human responses in particular murine responses are much more directed to domain III of E and complex conformational epitopes appear rare. Furthermore, we anticipate focussing the response to the EDE may require heterologous prime boosting strategies.

Dengue vaccines are now at an important juncture; a large scale Phase III trial has underperformed expectations and given a concerning safety signal of enhanced infection [5,38]. Here we have demonstrated the feasibility of locking the E-dimer to avoid generation of poorly neutralising antibodies such as those targeting immunodominant FLE. Together with the elimination of prM from an appropriate candidate subunit vaccine, this approach has the potential to generate broadly protecting subunit DENV/ZIKV vaccines.

Materials and methods

Cells, reagents and antibodies

The C6/36 cell line derived from mosquito *Aedes albopictus* was cultured in Leibovitz L-15 at 28°C. Vero and 293T cells were grown at 37°C in MEM and DMEM, respectively. All media were supplemented with 10% heat-inactivated fetal bovine serum (FBS), 100 units/ml penicillin, 100 μg/ml streptomycin and 2mM L-Glutamine. Monocyte-derived dendritic cells (MDDCs) were prepared as previously described[39].

2C8, a murine mAb directed to envelope domain III of DENV2 (EDIII), was a gift from Dr C. Puttikhunt and Dr. W. Kasinrerk (Biotec and Chiang Mai University Thailand). Alkaline phosphatase (ALP)-conjugated anti-human IgG (A9544), ALP-conjugated Streptavidin (S2890), p-nitrophenylphosphate (PNPP, N2770-50) and Bovine serum albumin (BSA, A7030) and polyethylenimine (408727) were purchased from Sigma. Strep Tactin-ALP conjugate (2-1503-001) was from IBA GmbH. Goat anti-mouse Igs-HRP (P0447) and Rabbit anti-human IgG-HRP (P0214) were from Dako. Luminata Classico Western HRP Substrate (WBLUC0100) was from Merk Millipore. MEM (31095) and Leibovitz L-15 (11415) were from Gibco, DMEM (D6046) was from Sigma and UltraDOMA-PF (12-727F) was from Lonza.

Virus stock

Dengue virus serotype 2 (16681) were grown in C6/36 cells and MDDCs. Cell-free supernatants were collected and stored at -80 °C. The titres of virus were determined by a focus forming assay on vero cells and expressed as focus-forming units (FFU) per ml[40]

Expression of human monoclonal anti-DENV E antibodies

A pair of plasmids containing the heavy and light chains of human IgG were co-transfected into 293T cells using the polyethylenimine method and cultured in protein-free media. Culture supernatants containing antibodies was harvested after 5 days. The abbreviation for anti-EDE1 mAbs 752-2C8 and 753(3)C10 were C8 and C10, respectively. The abbreviation for anti-EDE2 mAbs 747(4)A11 and 747(4)B7 were A11 and B7, respectively. The abbreviation for anti-FLE mAb 749B12was B12

sE direct ELISA

Purified DENV2 sE (WT, A259C or L107C/A313C) and BSA were used as coating antigen and negative control antigen respectively. NUNC immobilizer plates (436006) were coated with 50ul of 10ug/ml protein and blocked with 3% BSA. Plates were then incubated with 50 ul of 1 ug/ml of anti-FLE and anti-EDE mAbs supernatants followed by ALP-conjugated anti-human IgG. The activity was observed with PNPP and measured at 405 nm.

Determination of the ability of anti-EDE mAb to stabilize the E-dimer

A MAXISORP immunoplate (442404; NUNC) was coated with 50ul of 5ug/ml of human anti-FLE or anti-EDE mAbs. The plate was then blocked with 3% BSA for an hour followed by incubation with serial dilutions of Strep-tagged recombinant envelope protein DENV2. The reaction was visualized by AP-labelled Strep-Tactin and PNPP substrate. The reaction was stopped by adding NaOH and the absorbance was measured at 405nm.

Biochemical analyses

SEC-MALS was performed by loading ~150 ug of DENV2 FGA02 A259C protein into Superdex 200 10/300 GL column (GE life sciences) and samples were run in Tris 50 mM, NaCl 500 mM (pH 8.0) at a flow rate of 0.4 ml min-1. These samples passed through a Wyatt DAWN Heleos II EOS 18-angle laser photometer coupled to a Wyatt Optilab TrEX differential refractive index detector. Data was later analysed using Astra 6 software (Wyatt Technology Corp).

Analysis of the complex of DENV2 FGA02 WT along with Fab C8 and Fab A11 were performed in similar manner by loading 150 ug of DENV2 FGA02, 300 ug of Fab C8, 300 ug of Fab A11 and for complex formation a mixture of 150 ug of DENV2 FGA02 with 300ug of FabC8 and 150 ug of DENV2 FGA02 with 300 ug Fab A11. Proteins were injected using 100ul loop.

Ab competition ELISA

For mAb competition assays, DENV2 produced from C6/36 cell lines or MDDCs were captured onto MAXISORP immunoplates coated with 2C8; a mouse anti-EDIII mAb specific for DENV2, plates were then blocked with 3% BSA. An equal volume of fixed concentration of biotin labelled anti-FLE or anti-EDE mAbs at 1 ug/ml was mixed with a serial dilution of unlabelled anti-FLE, anti-EDE or irrelevant anti-Flu mAbs. The mixtures were then added to DENV captured to ELISA plates and incubated for 1 hr., following washing plates were then incubated with ALP-conjugated Streptavidin. The reaction was developed by the addition of PNPP substrate and stopped with NaOH. The absorbance was measured at 405 nm. For competitive ELISA, the signals are inversely proportional to the ability of unlabelled mAbs to compete with the biotin-labelled mAb for binding.

For the Ab displacement ELISA, biotin-labelled anti-FLE or anti-EDE mAbs was first added onto DENV captured to ELISA plates and incubated for 1 hr. After washing, unlabelled anti-FLE, anti-EDE or irrelevant anti-Flu mAbs was sequentially added and incubated for further 1, 5, 15, 30 and 60 mins. The reaction was then developed by adding ALP-conjugated Streptavidin and PNPP substrate. The ability of second unlabelled mAb to displace the binding of first biotin-labelled will yield a lower signal.

Measurement of prM cleavage on DENV

The efficiency of PrM cleavage was evaluated by running viral supernatants from C6/36 cell and DC on 12% SDS-PAGE and western blotting with mouse anti-E mAb (4G2) and human anti-prM (3-147) followed by a cocktail of goat anti-mouse Igs and rabbit anti-human IgG. Finally, the membrane was developed with chemiluminescence substrate. In addition, the levels of prM cleavage were also analyzed by detection of E and prM by ELISA[20]. Briefly viral supernatants from C6/36 and DC cells were captured onto plates coated with murine anti-E mAb (4G2). Then, E and prM were detected using a humanized version of 3H5 mAb (hu3H5) and human anti-prM (3-147), respectively.

Production and purification of wild type and disulphide stabilized sE proteins

Recombinant sE from different serotypes were cloned as previously described[22]. Single and double cysteine mutations were introduced by standard Gibson assembly cloning with primers containing mutant sequence and the mutation in constructs was verified by DNA sequencing. All

the constructs were transfected into Drosophila S2 cells and expressed as described previously[22]. All of the mutants as well as the WT protein produced different amounts of soluble aggregates that was removed by SEC. DENV2 WT and DENV2 A259C proteins were purified using affinity streptactin followed by SEC in 50 mM Tris (pH 8) and NaCl 500 mM. However, double disulphide bonded DENV2 L107C/A313C was observed to produced large amounts of soluble aggregate along with the dimer peaks in SEC after affinity chromatography and additional purification steps were introduced. DENV2 L107C/A313C mutant protein peak collected after affinity streptactin was adjusted to pH 8.5 with 100 mM Tris and to 2.5 M NaCl and bound to 1 ml hydrophobic interaction phenyl column. Protein was eluted using slow NaCl gradient from 2 M NaCl to 0 mM NaCl (30 column volumes). Mutant dimer protein eluted at 65.2 mS/ml conductance value in phenyl column purification conditions. This protein was further purified using SEC (in 50 mM Tris pH 8 500 mM NaCl).

DENV3 WT, DENV3 A257C and the DENV4 WT, DENV4 A259C mutant proteins were purified using the same protocol as for DENV2 WT and A259C stated above. DENV3 L107C/S311C and DENV4 L107C/A313C were purified using streptactin affinity chromatography followed by SEC purification (in 50 mM Tris pH 8, 200 mM NaCl) SDX200 column where the aggregates and monomer peaks were separated from the dimer peak. The dimer peak from both was subjected to another SEC (in 20 mM NaH2PO4, 250 mM NaCl and 20 mM disodium succinate, pH 7) for polishing. These purified proteins were buffer exchanged into Tris 50 mM and 500 mM NaCl and stored or used for assays. Yields of different proteins per litter of S2 cell culture are provided in Figures S3a.

Crystallization and three-dimensional structure determinations

Crystallization trials were performed in sitting drops of 400 nl. Drops were formed by mixing equal volumes of the protein and reservoir solution in the format of 96 Greiner plates, using a Mosquito robot, and monitored by a Rock-Imager. Crystals were optimized with a robotized Matrix Maker and Mosquito setups on 400 nl sitting drops, or manually in 24-well plates using 2–3 µL hanging drops at 18°C. The protein concentrations, crystallization and cryo-cooling conditions for diffraction data collection are listed in Supplementary Table 1. X-ray diffraction data were collected at beam lines PROXIMA-2 at the SOLEIL synchrotron (St Aubin, France), and ID29 at the European Synchrotron Radiation Facility (Grenoble, France). Diffraction data were processed using the XDS package and scaled with SCALA or AIMLESS[41] in conjunction with other programs of the CCP4 suite[42]. The high resolution limits for each structure were

determined using $CC_{1/2}$-based cutoffs of 0.30[43]. The structures were determined by molecular replacement with PHASER[44] using the search models listed in Supplementary Table 1.

Subsequently, careful model building with COOT[45], alternating with cycles of crystallographic refinement with the programs Phenix.Refine[46] and/or BUSTER/TNT[47], led to a final model. Refinement was constrained to respect non-crystallographic symmetry, and used target restraints and TLS refinement[48] (Supplementary Table 1). Electron density sharpening maps were computed with COOT and helped for manual model building[49]. Refined crystallographic models were analysed with MolProbity[50]. The figures were prepared using the PyMOL molecular Graphics System (Schrodinger)(pymol.sourceforge.net).

sE-liposomes co-flotation assay

Liposomes were prepared by freeze-thaw and extrusion through 100 nm pore size polycarbonate filters (Whatman 800309) using a 1:1:1:3 molar ratio of DOPC (1,2-dioleoyl-sn-glycero-3-phosphocholine) (850375C), DOPE (1,2-dioleoyl-sn-glycero-3-phos- phoethanolamine) (850725C), sphingomyelin (from bovine brain) (860062C), cholesterol (from ovine wool) (700000P) purchased from Avanti Polar Lipids. Purified sE (WT, A259C or L107C/A313C from DENV2 FGA-02 or DENV4 1-0093 and WT, A257C, L107C/S311C from DENV3 H87) was mixed with liposomes and incubated for 10 min at RT before overnight incubation at 30C under acidic conditions. The mixture was separated by ultracentrifugation on an Optiprep (Proteogenix 1114542) continuous 0-30% gradient. Aliquots from top and bottom fractions were analysed by western blot using an anti-strep tag antibody.

Figure Legends

Fig. 1. EDE mAbs can stabilize DENV envelope dimers.

a, binding of anti-FLE and anti-EDE mAbs to monomeric sE protein was determined by direct ELISA with sE coated to the ELISA plate. Results are expressed as mean of binding in arbitrary units (AU) from three independent experiments. The mAbs used in panel b are indicated by dots of the same colour.

b, The ability of selected mAbs to bind and assemble dimers was assessed by indirect ELISA. ELISA plates were coated with four anti-EDE mAbs and one anti-FLE mAb control, which binds monomeric sE. Plates were then incubated with a titration of soluble Strep-tagged sE monomer,

bound sE was revealed using ALP-labelled StrepTactin. The data are shown as mean±SEM from 3 independent experiments.

c, SEC/MALS analysis of isolated DENV2 sE, isolated Fab fragments and DENV2 sE with anti-EDE1 Fab C8 (left panel) and anti-EDE2 Fab A11 (right panel) mAbs. The molecular weight determined by MALS is indicated, corresponding to the y axis on the left. The UV absorbance was normalized such that the highest peak of each run is set to 1 (y axis on the right)

Fig. 2. Competition between anti-FLE and anti-EDE mAb.

a, Description of the schematic procedure of antibody replacement ELISA.

b&c, Competition for binding to dengue virions of anti-FLE mAb-B12, anti-EDE1 mAb-C10 and anti-EDE2 mAb A11. ELISA plates were coated with DENV2 virions produced in C6/36 cells (high prM) (b) and DC (low prM) (c) captured by murine mAb 2C8 which binds to EDIII of DENV2. Plates were then incubated with a pair of antibodies; one of which was biotinylated at a concentration of 1µg/ml and a second antibody which was added in increasing concentrations. Binding of biotinylated antibody was revealed by ALP-conjugated Streptavidin. The data are shown as mean±SEM from 3 independent experiments.

Fig. 3. Engineering covalently linked E-dimers.

a, Localization of the residues identified by MODIP susceptible to form inter-chain disulphide bonds upon mutation to cysteine. The sE dimer is shown is coloured by subunit, with the MODIP residue pairs indicated in the corresponding colours. A disulphide bond is modelled and is shown as green sticks. The MODIP score, indicated for each residue pair, is a measure of favourability of the geometry of the selected amino acids for disulphide bond formation where A is best and D is worst.

b, Histogram showing the approximate yields in mg per litre of S2 cell culture of DENV2 FGA02 sE protein eluting as monomer, dimer and aggregates separated by SEC for wild type and for the four cysteine mutants presented in panel a. The yields of covalent dimers are shown in green bars (highlighted with green arrows when sufficient yields for further studies were obtained).

c, MALS analysis of DENV2 A259C sE (red trace). The fractions eluting as dimer in a first step of SEC (which eliminated monomers and aggregates) was re-run by SEC and then superposed to the elution profile of DENV2 WT sE (blue trace). The UV absorbance was normalized such that

the highest peak of each run is set to 1 (y axis on the right). The molecular weight determined by MALS is indicated, corresponding to the y axis on the left.

d, SEC elution profile of L107C/A313C sE superposed to that of A259C sE, showing that the peaks are at the same elution volume, which corresponds to a dimer characterized by MALS in panel (b). As in (c) the peaks corresponding to monomer and aggregates were eliminated in an initial SEC run.

e, Coomassie stained SDS-PAGE run of sE WT and sE mutants of DENV2 (in the absence (-) or presence (+) of reducing agent DTT). The black arrow indicates the bands of the disulphide stabilized sE dimer.

Fig. 4. Structures of DENV2 sE FGA02 WT and mutants in complex with anti-EDE2 Fab A11.

a, The previously determined structure of DENV2 sE WT in complex with EDE2 A11 Fab (PDB code 4UTB). The molecular 2-fold axis is shown as a light-brown central rod, and the cysteines are displayed as green spheres. The heavy and light chains of Fab A11 are colored in green and light grey, respectively. sE proteins are color-coded by domains: domain I - red, domain II - yellow and domain III - blue.

b,c Structures determined here of DENV2 sE A259C mutant in complex with anti-EDE2 A11 Fab (b) and DENV2 sE L107/A313C mutant in complex with anti-EDE2 A11 Fab (c). The constant domains of the two Fab A11 in DENV2 sE A259C complex were disordered in the final structure and thereby are shown in transparent ribbons. Lower panels b and c : zoom views of the engineered disulfides are shown respectively for DENV2 sE A259C in complex with anti-EDE2 A11 Fab and DENV2 sE L107/A313C in complex with anti-EDE2 A11 Fab.

Fig. 5. Covalently linked sE dimers recapitulate the EDE and do not interact with liposomes.

a,b ELISA plates were coated with DENV2 either wild type monomeric sE (sE WT) or the two covalently linked sE dimers (a) A259C or (b) L107C/A313C and following incubation with panel of anti-EDE1 and anti-EDE2 mAbs (left panel) or anti-FLE at 1 ug/ml (right panel), binding was determined using ALP-conjugated anti-human IgG.

c, Results of co-flotation with liposomes in an Optiprep gradient at low pH (see Methods for lipid composition). Wild type, single and double mutants from DENV2 FGA02, DENV3 H86 and DENV4 1-0093 were incubated at pH 5.8 with liposomes and run in an Optiprep gradient. Insertion of the WT sE proteins in the liposome membrane results in its floatation to the low

density top (T) fractions of the gradient (lanes 1). A fraction of the single mutants appears to still be able to float with the liposomes (lanes 3), whereas in the double mutants, there is no sE protein recovered from the top fraction (lanes 5), in line with the fact that the FLE is not exposed.

Supplementary Figure 1. prM cleavage in C6/36 and DC produced DENV2

(a) The efficiency of PrM cleavage was evaluated by Western blot. C6/36 cell and DC produced virions were run on 12% SDS-PAGE blotted and probed with mouse anti-E mAb (4G2) and human anti-prM (3-147) followed by a cocktail of goat anti-mouse Igs and rabbit anti-human IgG. Finally, the membrane was developed with chemiluminescence substrate.
b)The levels of prM cleavage were also analyzed by detection of E and prM by ELISA. Briefly viral supernatants from C6/36 and DC cells were captured onto plates coated with anti-E mAb (4G2). Then, E and prM were detected by using a humanized version of 3H5 mAb (hu3H5) and human anti-prM (3-147), respectively. Values are shown as mean±SEM

Supplementary Figure 2. Anti-FLE and anti-EDE mAbs stably bound to DENV.

a, Description of the schematic procedure of Antibody replacement ELISA.
b&c, Once bound anti-FLE and anti-EDE mAbs cannot be replaced. Biotinylated antibody was bound to DENV2 particles captured by murine anti-DENV2 EDIII mAb, 2C8, and following washing were incubated with unconjugated competitor antibodies following incubation for the indicated times residual biotin-conjugated mAb was revealed with ALP-conjugated Streptavidin. The data are shown as mean±SEM from 3 independent experiments.

Supplementary Figure 3. Recombinant DENV sE protein yield.

a, Histograms showing approximate yields of monomer, dimer and soluble aggregates during SEC for wild type and two stabilized cysteine mutants of sE from DENV1 Hawaii strain, DENV2 16681 strain, DENV3 H87 strain and DENV4 1-0093 strain are depicted.
b, Coomassie stained SDS PAGE analysis of sE WT and mutants of DENV3 and DENV4 (in absence (-) or in presence (+) of reducing agent DTT). The black arrow on the right indicates the bands of the disulphide stabilized sE dimer.
c, SEC profile of purified single (red trace) and double cysteine (black trace) sE mutants from DENV3 H87 (left panel) and DENV4 1-0093 (right panel) is shown in superimposition to the DENV2 FGA02 A259C mutant (green dotted trace).

Supplementary Figure 4. Localization of disulphides in DENV2 sE mutants in complex with EDE2 Fab A11.

a,b Difference map around the mutation sites of A259C (left panel) and of L107C/A313C (right panel) structures, calculated from the experimental structure factor amplitudes using phases of the WT 4UTB structure from which the cysteine residues are not present. The green grids represent extra density indicating the presence of disulfides. The peak around residue 259 is observed at 5.6 sigma. The two peaks around residues 107 and 313 in both sE protomers have heights of 6 and 5.1 sigma, respectively.

b, Electron density 2Fo-Fc maps displaying regions around C259, in the A259C sE mutant (left panel on top) and between C107 and C313 in the L107C/A313C sE mutant (right panel on top). Fo and Fc are amplitudes of the structure factures measured and calculated from the final refined model, respectively, for each reflection. The phases are derived from the final model weighed by the agreement between Fo and Fc, and the standard deviation of the measured Fo. Bfactor sharpening applied on the top panels 2Fo-Fc maps are shown in the lower panels for both structures where the engineered Cys positions are depicted in green sticks (see Methods).

Supplementary Figure 5. Superposition of sE dimers from DENV2 sE WT and from DENV2 sE Cys mutants in complex with Fab A11.

Superposition of carbon alpha structures of sE dimer from DENV2 sE WT-Fab A11 structure (4UTB) (shown in green) with sE dimer from DENV2 sE A259C mutant (left panel, in red) and sE dimer from DENV2 L107C/A313C sE mutant (right panel, in red). The table shows the RMSD scores (Å) with the number of Cα atoms used shown in bracket.

Reference:

1. Screaton, G., Mongkolsapaya, J., Yacoub, S. & Roberts, C. New insights into the immunopathology and control of dengue virus infection. *Nat Rev Immunol* **15**, 745-759 (2015).
2. Bhatt, S.*, et al.* The global distribution and burden of dengue. *Nature* **496**, 504-507 (2013).
3. Guzman, M.G., Gubler, D.J., Izquierdo, A., Martinez, E. & Halstead, S.B. Dengue infection. *Nat Rev Dis Primers* **2**, 16055 (2016).
4. Simmons, C.P., Farrar, J.J., Nguyen v, V. & Wills, B. Dengue. *N Engl J Med* **366**, 1423-1432 (2012).
5. World Health Organization (WHO) Strategic Advisory Group of Experts. Dengue vaccine:

http://www.who.int/immunization/sage/meetings/2016/april/SAGE_April_2016_Meeting_Web_summary.pdf?ua=1. (2016).
6. Barba-Spaeth, G.*, et al.* Structural basis of potent Zika-dengue virus antibody cross-neutralization. *Nature* **536**, 48-53 (2016).
7. Guzman, M.G., Alvarez, M. & Halstead, S.B. Secondary infection as a risk factor for dengue hemorrhagic fever/dengue shock syndrome: an historical perspective and role of antibody-dependent enhancement of infection. *Arch Virol* **158**, 1445-1459 (2013).
8. Halstead, S.B. Neutralization and antibody-dependent enhancement of dengue viruses. *Advances in virus research* **60**, 421-467 (2003).
9. Beltramello, M.*, et al.* The human immune response to Dengue virus is dominated by highly cross-reactive antibodies endowed with neutralizing and enhancing activity. *Cell Host Microbe* **8**, 271-283 (2010).
10. de Alwis, R.*, et al.* In-depth analysis of the antibody response of individuals exposed to primary dengue virus infection. *PLoS Negl Trop Dis* **5**, e1188 (2011).
11. De Alwis, R.*, et al.* Identification of human neutralizing antibodies that bind to complex epitopes on dengue virions. *Proc Natl Acad Aci U S A* **109**, 7439-7444 (2012).
12. Dejnirattisai, W.*, et al.* A new class of highly potent, broadly neutralizing antibodies isolated from viremic patients infected with dengue virus. *Nat Immunol* **16**, 170-177 (2015).
13. Fibriansah, G.*, et al.* A potent anti-dengue human antibody preferentially recognizes the conformation of E protein monomers assembled on the virus surface. *EMBO molecular medicine* **6**, 358-371 (2014).
14. Smith, S.A.*, et al.* Human monoclonal antibodies derived from memory B cells following live attenuated dengue virus vaccination or natural infection exhibit similar characteristics. *J Infect Dis* **207**, 1898-1908 (2013).
15. Teoh, E.P.*, et al.* The Structural Basis for Serotype-Specific Neutralization of Dengue Virus by a Human Antibody. *Science translational medicine* **4**, 139ra183-139ra183 (2012).
16. Priyamvada, L.*, et al.* Human antibody responses after dengue virus infection are highly cross-reactive to Zika virus. *Proc Natl Acad Sci U S A* **113**, 7852-7857 (2016).
17. Oliphant, T.*, et al.* Antibody recognition and neutralization determinants on domains I and II of West Nile Virus envelope protein. *J Virol* **80**, 12149-12159 (2006).
18. Balsitis, S.J.*, et al.* Lethal antibody enhancement of dengue disease in mice is prevented by Fc modification. *PLoS Pathog* **6**, e1000790 (2010).
19. Rodenhuis-Zybert, I.A.*, et al.* A fusion-loop antibody enhances the infectious properties of immature flavivirus particles. *J Virol* **85**, 11800-11808 (2011).
20. Dejnirattisai, W.*, et al.* Cross-reacting antibodies enhance dengue virus infection in humans. *Science* **328**, 745-748 (2010).
21. Dejnirattisai, W.*, et al.* Dengue virus sero-cross-reactivity drives antibody-dependent enhancement of infection with zika virus. *Nat Immunol* **17**, 1102-1108 (2016).
22. Rouvinski, A.*, et al.* Recognition determinants of broadly neutralizing human antibodies against dengue viruses. *Nature* **520**, 109-113 (2015).
23. Cherrier, M.V.*, et al.* Structural basis for the preferential recognition of immature flaviviruses by a fusion-loop antibody. *EMBO J* **28**, 3269-3276 (2009).

24. Dai, L., *et al.* Structures of the Zika Virus Envelope Protein and Its Complex with a Flavivirus Broadly Protective Antibody. *Cell Host Microbe* **19**, 696-704 (2016).
25. Thangudu, R.R., *et al.* Native and modeled disulfide bonds in proteins: knowledge-based approaches toward structure prediction of disulfide-rich polypeptides. *Proteins* **58**, 866-879 (2005).
26. Wengler, G., Wengler, G. & Rey, F.A. The isolation of the ectodomain of the alphavirus E1 protein as a soluble hemagglutinin and its crystallization. *Virology* **257**, 472-482 (1999).
27. Modis, Y., Ogata, S., Clements, D. & Harrison, S.C. Structure of the dengue virus envelope protein after membrane fusion. *Nature* **427**, 313-319 (2004).
28. Messer, W.B., *et al.* Functional Transplant of a Dengue Virus Serotype 3 (DENV3)-Specific Human Monoclonal Antibody Epitope into DENV1. *J Virol* **90**, 5090-5097 (2016).
29. Cockburn, J.J., *et al.* Mechanism of dengue virus broad cross-neutralization by a monoclonal antibody. *Structure* **20**, 303-314 (2012).
30. Fibriansah, G., *et al.* DENGUE VIRUS. Cryo-EM structure of an antibody that neutralizes dengue virus type 2 by locking E protein dimers. *Science* **349**, 88-91 (2015).
31. Fibriansah, G., *et al.* A highly potent human antibody neutralizes dengue virus serotype 3 by binding across three surface proteins. *Nat Commun* **6**, 6341 (2015).
32. Junjhon, J., *et al.* Influence of pr-M cleavage on the heterogeneity of extracellular dengue virus particles. *Journal of virology* **84**, 8353-8358 (2010).
33. Dowd, K.A., Jost, C.A., Durbin, A.P., Whitehead, S.S. & Pierson, T.C. A dynamic landscape for antibody binding modulates antibody-mediated neutralization of West Nile virus. *PLoS Pathog* **7**, e1002111 (2011).
34. Fibriansah, G., *et al.* Structural Changes in Dengue Virus When Exposed to a Temperature of 37C. *J Virol* **87**, 7585-7592 (2013).
35. Zhang, X., *et al.* Dengue structure differs at the temperatures of its human and mosquito hosts. *Proc Natl Acad Sci U S A* **110**, 6795-6799 (2013).
36. Goo, L., *et al.* Zika Virus Is Not Uniquely Stable at Physiological Temperatures Compared to Other Flaviviruses. *mBio* **7**, e01396-01316 (2016).
37. Kostyuchenko, V.A., *et al.* Structure of the thermally stable Zika virus. *Nature* **533**, 425-428 (2016).
38. Hadinegoro, S.R., *et al.* Efficacy and Long-Term Safety of a Dengue Vaccine in Regions of Endemic Disease. *N Engl J Med* **373**, 1195-1206 (2015).
39. Dejnirattisai, W., *et al.* A complex interplay among virus, dendritic cells, T cells, and cytokines in dengue virus infections. *The Journal of Immunology* **181**, 5865-5874 (2008).
40. Sittisombut, N., *et al.* Lack of augmenting effect of interferon-gamma on dengue virus multiplication in human peripheral blood monocytes. *J Med Virol* **45**, 43-49 (1995).
41. Evans, P.R. & Murshudov, G.N. How good are my data and what is the resolution? *Acta Crystallogr D Biol Crystallogr* **69**, 1204-1214 (2013).
42. Winn, M.D., *et al.* Overview of the CCP4 suite and current developments. *Acta Crystallogr D Biol Crystallogr* **67**, 235-242 (2011).
43. Karplus, P.A. & Diederichs, K. Assessing and maximizing data quality in macromolecular crystallography. *Curr Opin Struct Biol* **34**, 60-68 (2015).

44. McCoy, A.J.*, et al.* Phaser crystallographic software. *J Appl Crystallogr* **40**, 658-674 (2007).
45. Emsley, P., Lohkamp, B., Scott, W.G. & Cowtan, K. Features and development of Coot. *Acta Crystallogr D Biol Crystallogr* **66**, 486-501 (2010).
46. Afonine, P.V.*, et al.* Towards automated crystallographic structure refinement with phenix.refine. *Acta Crystallogr D Biol Crystallogr* **68**, 352-367 (2012).
47. Blanc, E.*, et al.* Refinement of severely incomplete structures with maximum likelihood in BUSTER-TNT. *Acta Crystallogr D Biol Crystallogr* **60**, 2210-2221 (2004).
48. Winn, M.D., Murshudov, G.N. & Papiz, M.Z. Macromolecular TLS refinement in REFMAC at moderate resolutions. *Methods Enzymol* **374**, 300-321 (2003).
49. Liu, C. & Xiong, Y. Electron density sharpening as a general technique in crystallographic studies. *J Mol Biol* **426**, 980-993 (2014).
50. Chen, V.B.*, et al.* MolProbity: all-atom structure validation for macromolecular crystallography. *Acta Crystallogr D Biol Crystallogr* **66**, 12-21 (2010).

Acknowledgements: We thank Watchara Kasinrerk and Chunya Putthikhunt for anti-dengue anti-DomIII mAb 2C8; J. Freire and G. Bowler for help and discussion; the staff at the crystallogenesis and chemogenomic & biological screening facilities at Institut Pasteur; the staff at beamline PX2 at SOLEIL synchrotron (Saclay, France), the staff at beamline ID29 at the European Synchrotron Radiation Facility (Grenoble, France); Fabrice Agou on Institute Pasteur for the MALS system. We acknowledge support from the European Commission FP7 Programme for the DENFREE project under Grant Agreement number 282 378FP7 (F.A.R., J.M., and G.R.S.); the "Integrative Biology of Emerging Infectious Diseases" Labex (Laboratoire d'Excellence) grant number ANR-10-LABX-62-IBEID (French Government's "Investissements d'Avenir" program) (F.A.R.); the Medical Research Council, UK (J.M.); the National Institute for Health Research Biomedical Research Centre, Funding Scheme, UK (G.R.S.); and the NEUTRAVIR grant from Région Ile-de-France (DIM-Maladies Infectieuses) (F.A.R.). G.R.S. is a Wellcome Trust Senior Investigator.

Author contributions: FAR, GRS and JM designed the experiments, PGC, FAR and AR designed the cysteine mutants; AR and AS produced and purified the recombinant DENV2-3-4 sE proteins and the antibody fragment A11; WD, PS and WW produced antibodies and performed binding experiments; AR grew the crystals and collected synchrotron data together with MCV; MCV, PGC and SD processed the data, built, refined and analysed the atomic models. AR and PGC made the MALS experiments; GBS did the floatation experiments with liposomes. GRS and FAR wrote the paper with the help of JM, GBS, AR, MCV, WD, and PGC.

Author Information. Coordinates and structure factors amplitudes have been deposited in the Protein Data Bank under accession numbers 5N0A and 5N09 for DENV2 sE A259C and DENV2 sE L107C/A313C mutants in complex with EDE2 A11 Fab complexes, respectively.

COMPETING FINANCIAL INTERESTS

The EDE antibodies, EDEepitope and envelope protein dimers that induce EDE antibodies are the subject of a patent application by Imperial College and Institute Pasteur on which G.S., J.M., F.R., A.R. and G.B.S. are named as inventors.

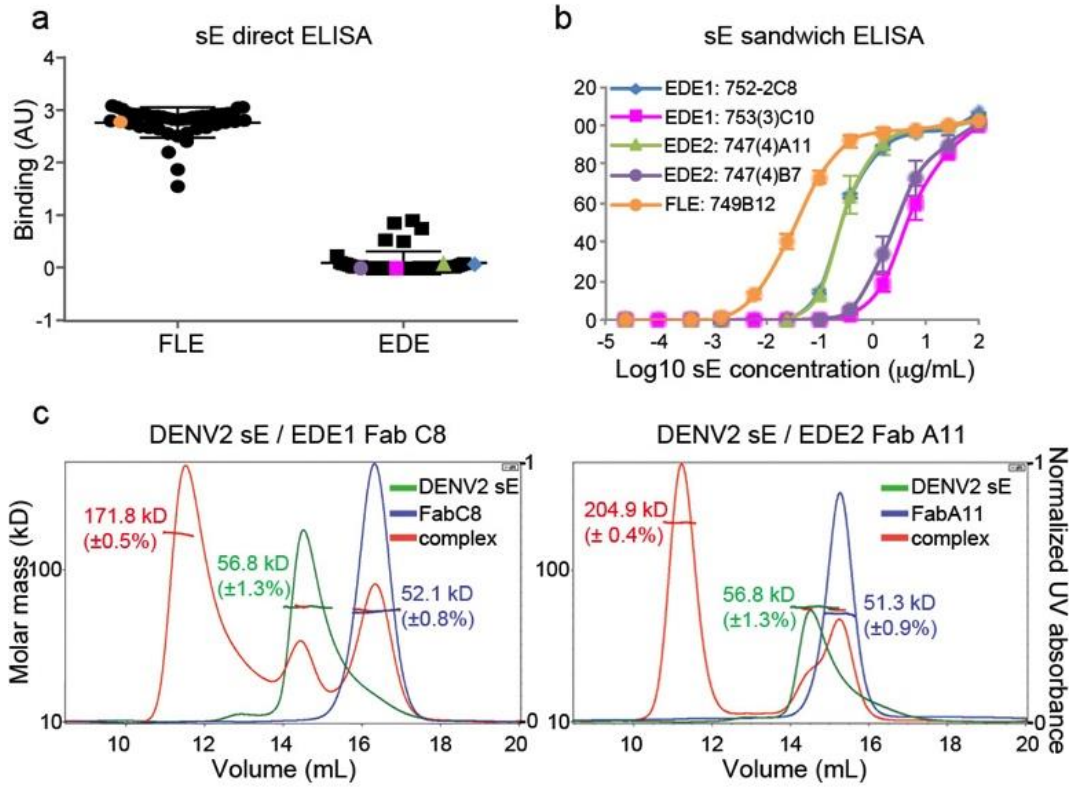
a
sE direct ELISA
Binding (AU)
FLE
EDE
b
sE sandwich ELISA
EDE1: 752-2C8
EDE1: 753(3)C10
EDE2: 747(4)A11
EDE2: 747(4)B7
FLE: 749B12
Log10 sE concentration (μg/mL)
c
DENV2 sE / EDE1 Fab C8
171.8 kD (±0.5%)
56.8 kD (±1.3%)
52.1 kD (±0.8%)
DENV2 sE
FabC8
complex
Molar mass (kD)
Volume (mL)
DENV2 sE / EDE2 Fab A11
204.9 kD (± 0.4%)
56.8 kD (±1.3%)
51.3 kD (±0.9%)
DENV2 sE
FabA11
complex
Volume (mL)
Normalized UV absorbance

Figure 1

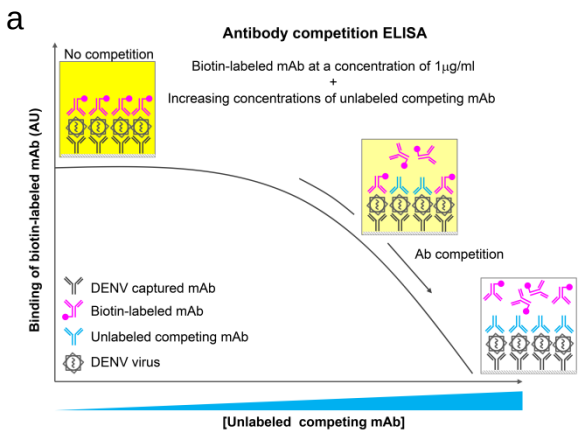
a
Antibody competition ELISA
No competition
Biotin-labeled mAb at a concentration of 1µg/ml
+
Increasing concentrations of unlabeled competing mAb
Binding of biotin-labeled mAb (AU)
Ab competition
DENV captured mAb
Biotin-labeled mAb
Unlabeled competing mAb
DENV virus
[Unlabeled competing mAb]

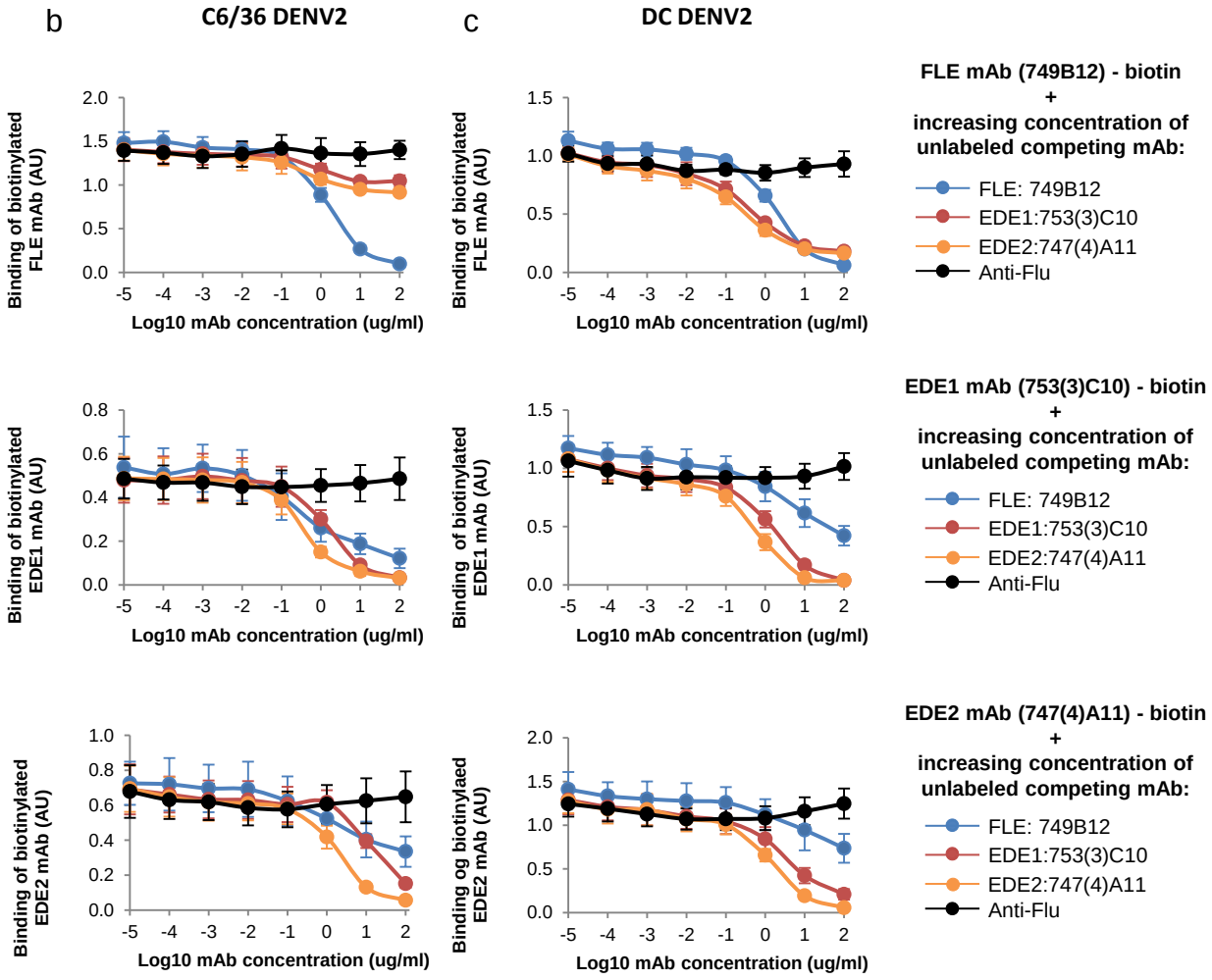
b
C6/36 DENV2
c
DC DENV2
Binding of biotinylated FLE mAb (AU)
Binding of biotinylated EDE1 mAb (AU)
Binding of biotinylated EDE2 mAb (AU)
Binding og biotinylaed EDE2 mAb (AU)
Log10 mAb concentration (ug/ml)
FLE mAb (749B12) - biotin
+
increasing concentration of unlabeled competing mAb:
FLE: 749B12
EDE1:753(3)C10
EDE2:747(4)A11
Anti-Flu
EDE1 mAb (753(3)C10) - biotin
+
increasing concentration of unlabeled competing mAb:
FLE: 749B12
EDE1:753(3)C10
EDE2:747(4)A11
Anti-Flu
EDE2 mAb (747(4)A11) - biotin
+
increasing concentration of unlabeled competing mAb:
FLE: 749B12
EDE1:753(3)C10
EDE2:747(4)A11
Anti-Flu

Figure 2

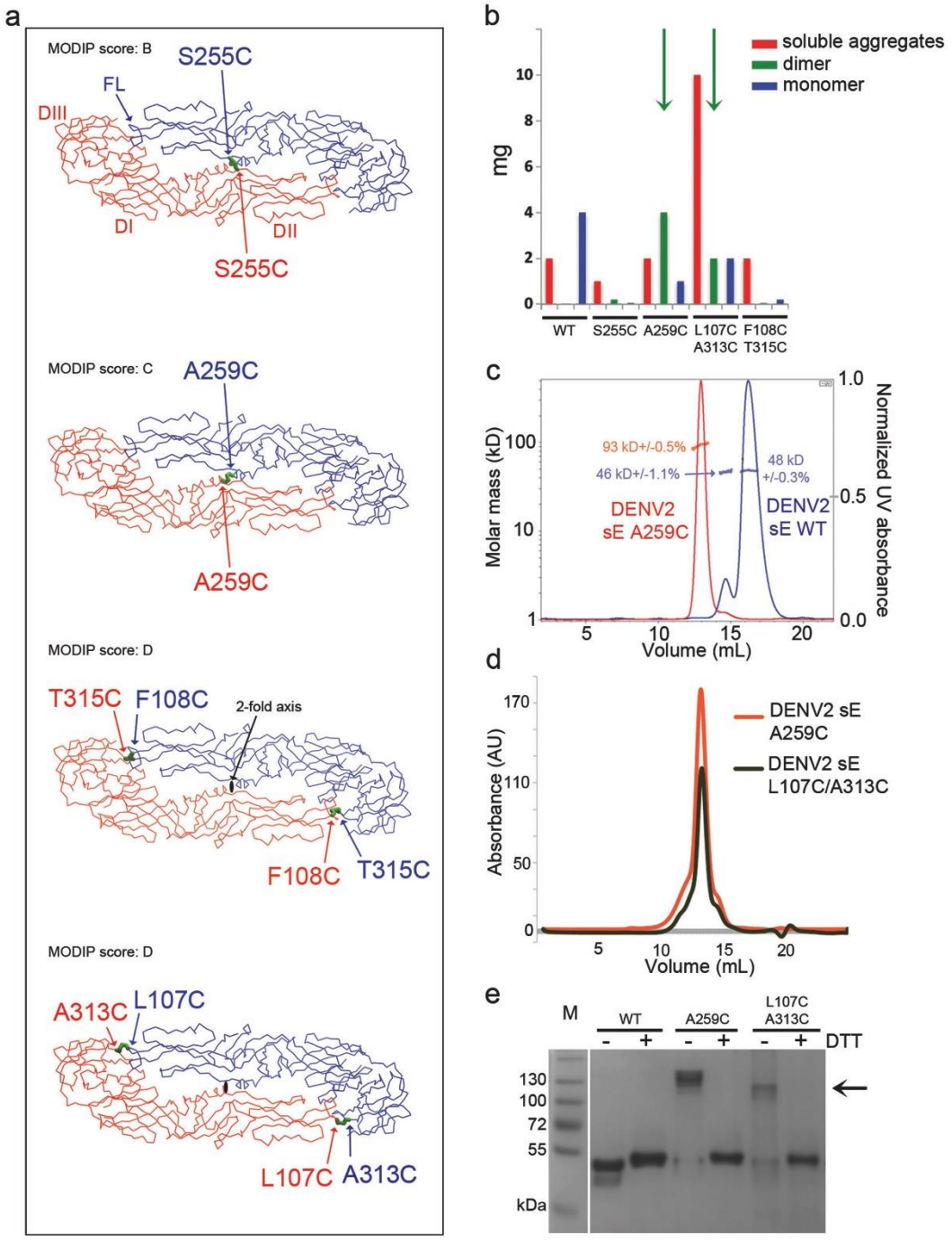
a
MODIP score: B
S255C
FL
DIII
DI
DII
S255C
MODIP score: C
A259C
A259C
MODIP score: D
T315C
F108C
2-fold axis
F108C
T315C
MODIP score: D
A313C
L107C
L107C
A313C
b
soluble aggregates
dimer
monomer
mg
WT
S255C
A259C
L107C A313C
F108C T315C
c
Molar mass (kD)
Normalized UV absorbance
93 kD+/-0.5%
46 kD+/-1.1%
48 kD +/-0.3%
DENV2 sE A259C
DENV2 sE WT
Volume (mL)
d
Absorbance (AU)
DENV2 sE A259C
DENV2 sE L107C/A313C
Volume (mL)
e
M
WT
A259C
L107C A313C
DTT
kDa

Figure 3

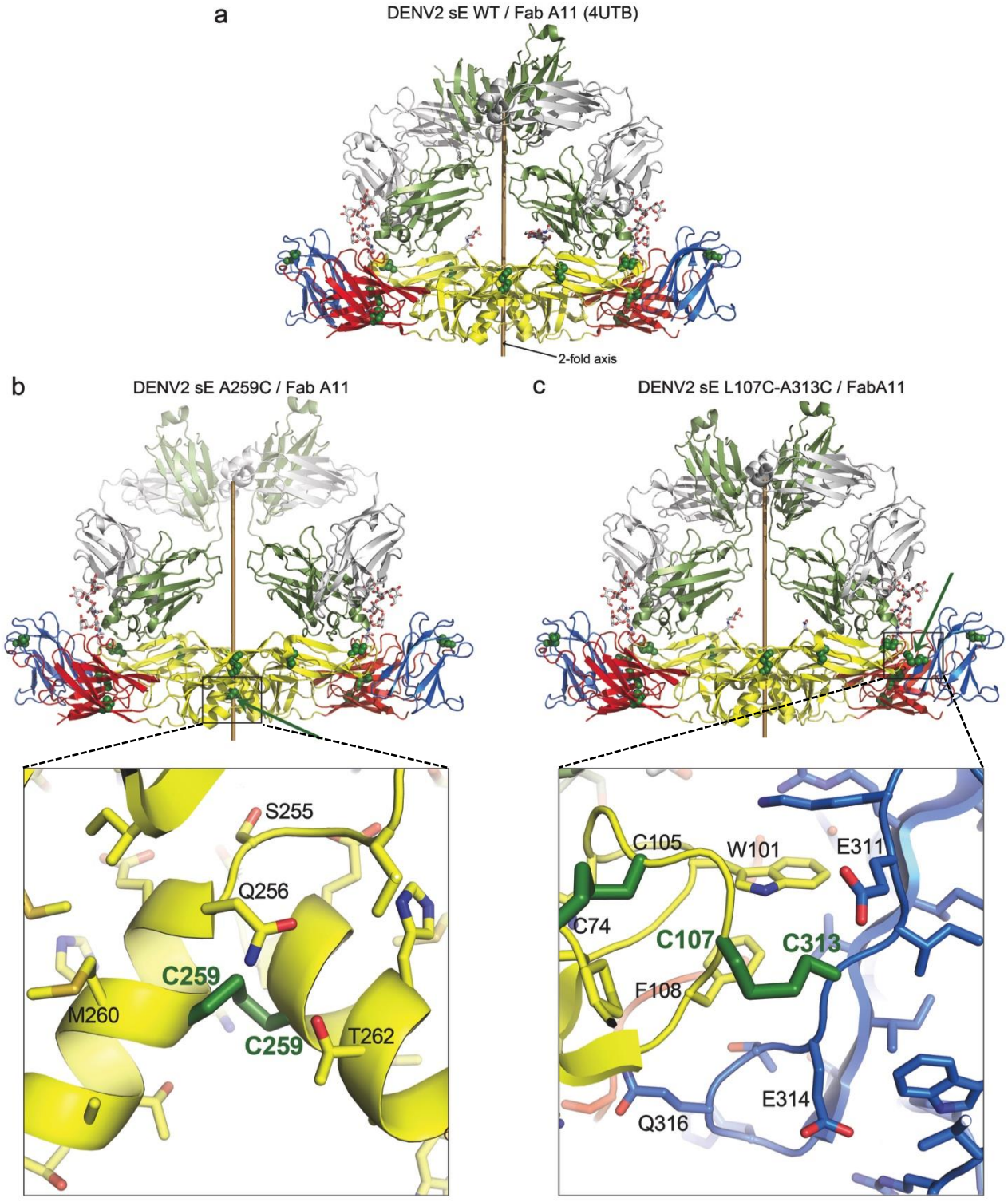
a
DENV2 sE WT / Fab A11 (4UTB)
2-fold axis
b
DENV2 sE A259C / Fab A11
S255
Q256
C259
M260
C259
T262
c
DENV2 sE L107C-A313C / FabA11
C105
W101
E311
C74
C107
C313
F108
E314
Q316

Figure 4

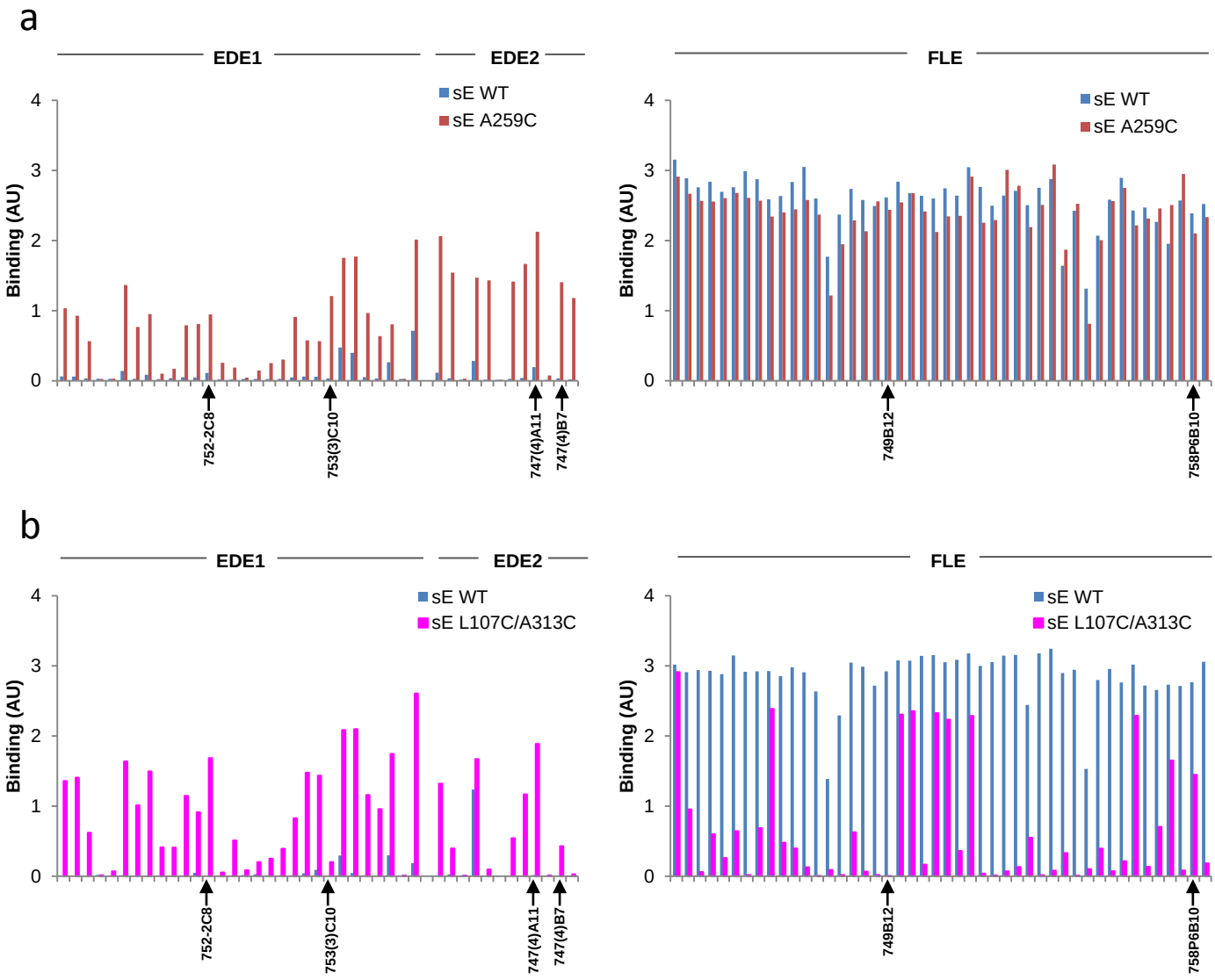
a
EDE1
EDE2
FLE
sE WT
sE A259C
Binding (AU)
0
1
2
3
4
752-2C8
753(3)C10
747(4)A11
747(4)B7
749B12
758P6B10
b
sE L107C/A313C

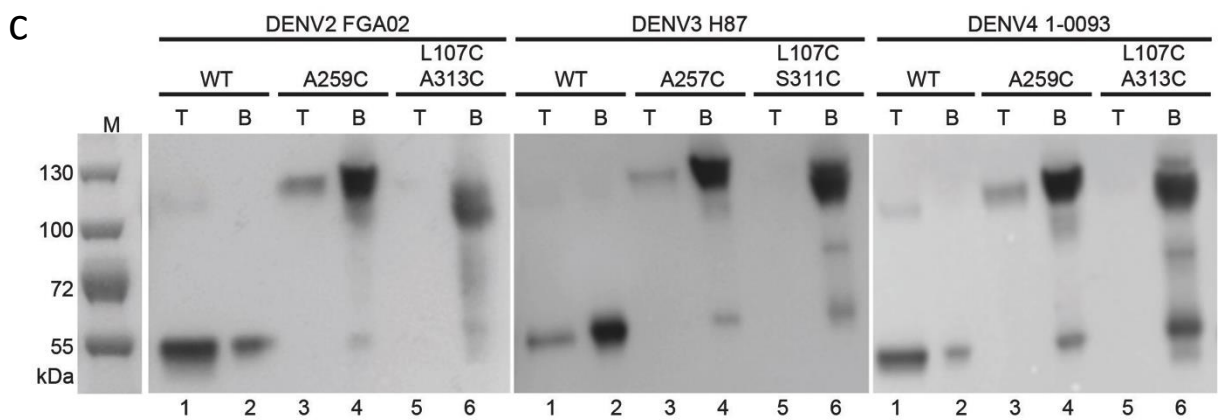
c
DENV2 FGA02
DENV3 H87
DENV4 1-0093
WT
A259C
L107C
A313C
A257C
S311C
T
B
M
130
100
72
55
kDa
1
2
3
4
5
6

Figure 5

a

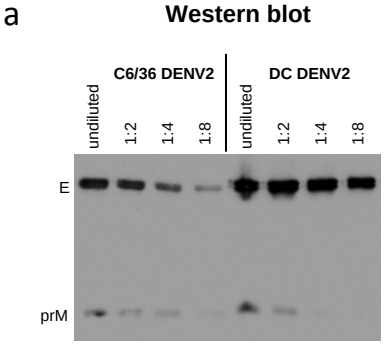

b

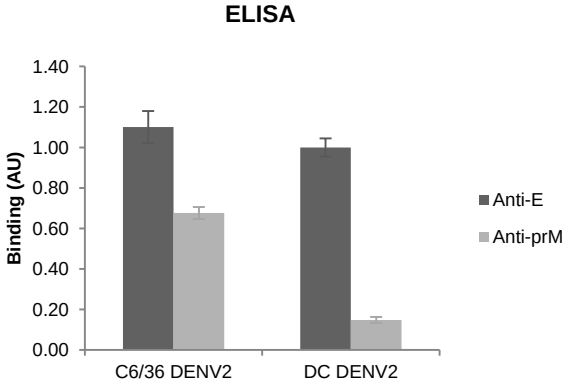

Supplementary Figure1

a

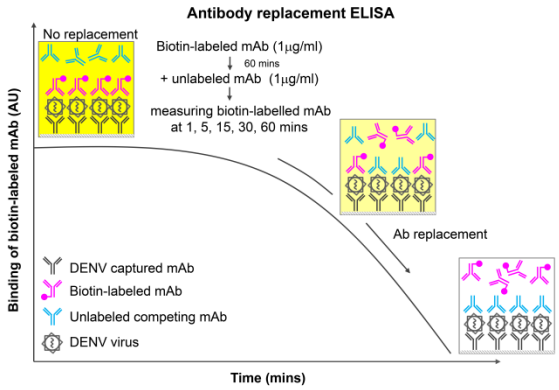

c

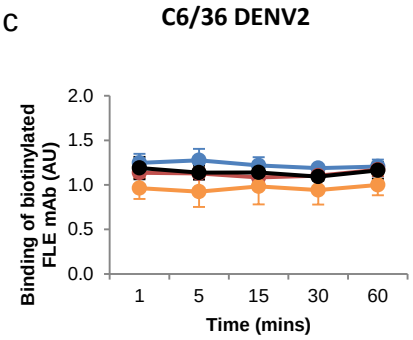

d

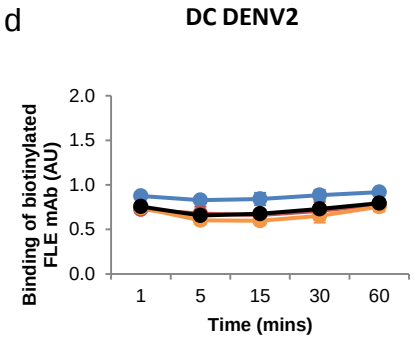

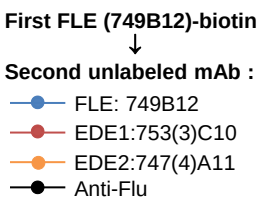

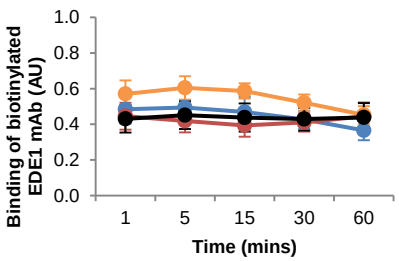

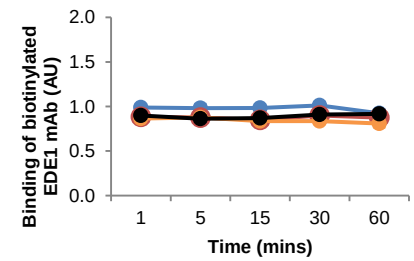

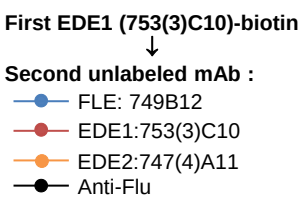

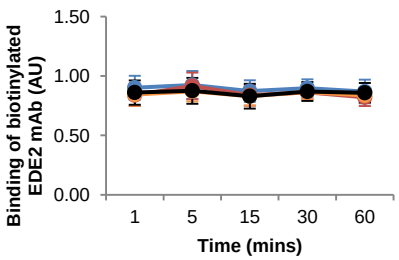

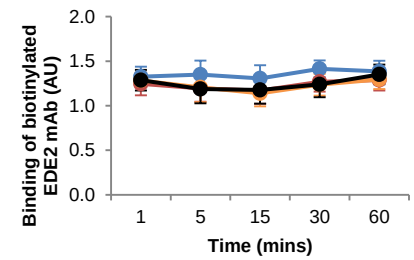

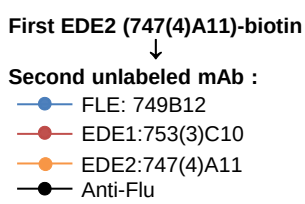

Supplementary Figure2

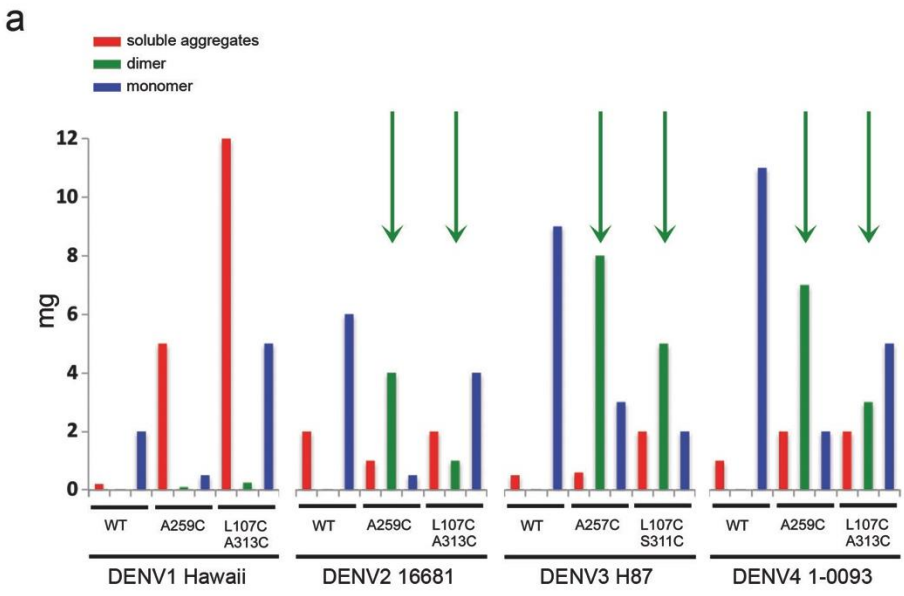

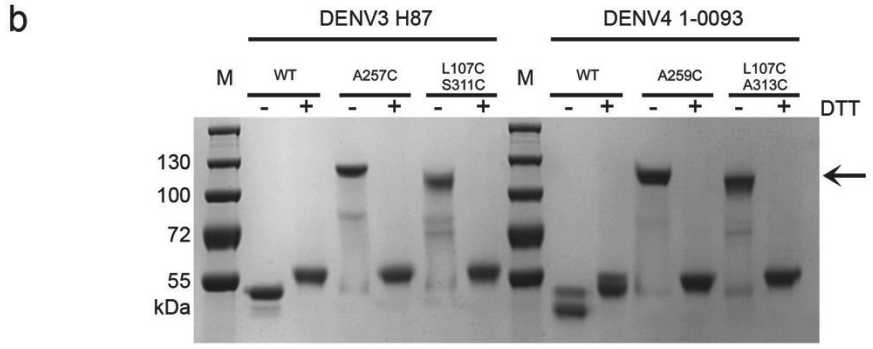

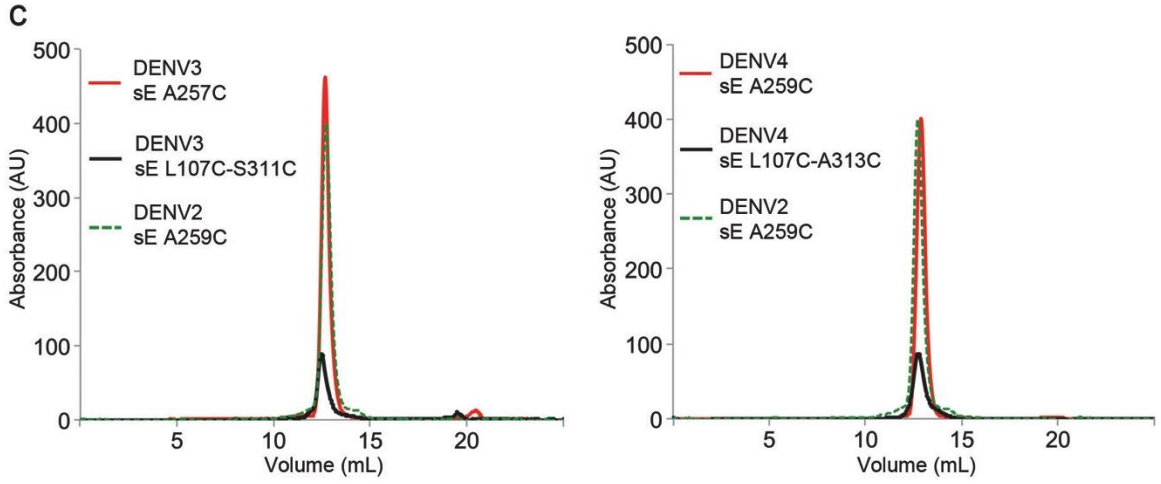

Supplementary Figure 3

DENV2 sE A259C / Fab A11

DENV2 sE L107C-A313C / Fab A11

a. Fo-Fc maps

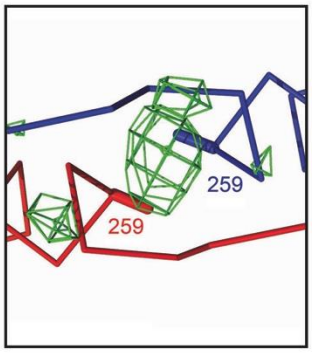

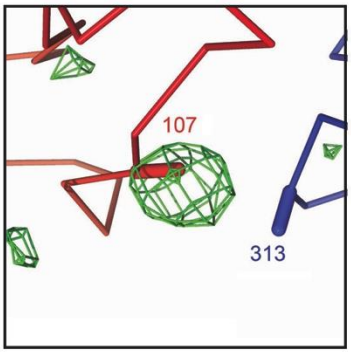

b. 2Fo-Fc maps

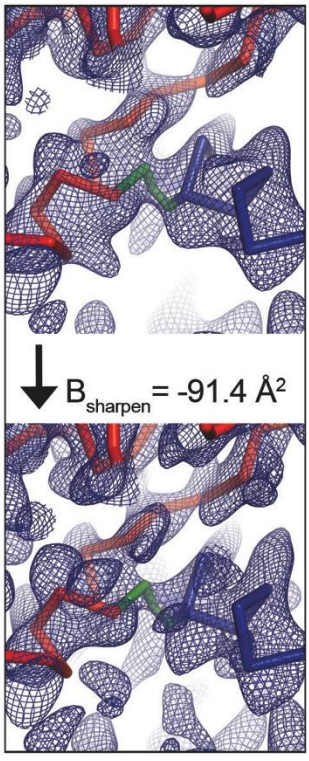

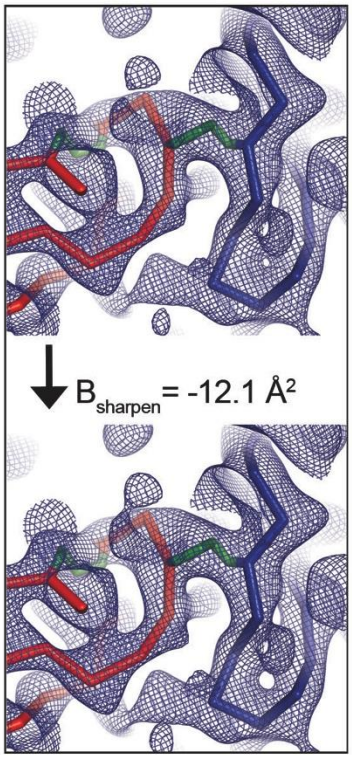

Supplementary Figure 4

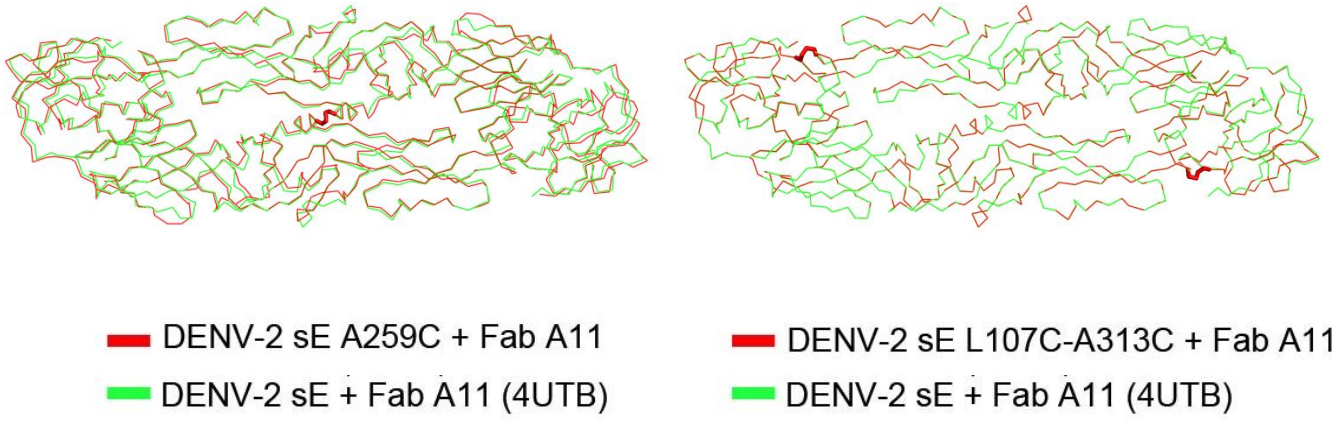

RMSD of aligned E dimer Cα atoms (Å)	**DENV2-A259C-Fab A11**	**DENV2-L107C-A313C-Fab A11**
DENV2-Fab A11 (4UTB)	1.11 (775)	0.14 (775)

Supplementary Figure 5

Supplementary Table 1. Crystallization conditions, data collection and refinement statistics.

Structure	DENV2 sE A259C - EDE2 A11 Fab fragment	DENV2 sE L107C/A313C - EDE2 A11 Fab fragment
PDB code	5N0A	5N09
Crystallization conditions		
Protein concentration (mg/ml)*	0.6	0.4
Crystallization buffer	100mM Hepes pH 7.5 19% PEG 6K, 1.5% (v/v) MPD	100mM Tris pH 8.5 20.7% PEG 4K
Cryoprotectant	16% glycerol in 67% of crystallization condition	16% ethylene glycol in 67% of crystallization condition
Data Collection‡		
Synchrotron beamline/Detector	SOLEIL PX2 / Eiger 9M	ESRF ID29 / Pilatus 6M
Space group	P 2_1 2_1 2	P 2_1 2_1 2
Unit cell a, b, c (Å); α, β, γ (°)	182.3, 208.7, 58.8; 90, 90, 90	180.6, 205, 58.9; 90, 90, 90
Resolution (Å)	50-**3.9** (4.1-3.9)	50-**3.9** (4.3-3.9)
Anisotropy directions‡‡		
Resolution where $CC_{1/2}$ > 0.30		
overall (Å)	**3.9**	**3.9**
along h axis (Å)	**3.9**	**3.9**
along k axis (Å)	7.2	6.2
along l axis (Å)	**3.9**	**3.9**
Measured reflections	77 520 (18 336)	101 266 (23 344)
Unique reflections	20 282 (4 789)	19 970 (4 741)
Mn(I) half-set correlation (%)	94.9 (68.2)	89.1 (50.8)
Mean I/σ(I)	3.1 (1.4)	2.4 (0.7)
Completeness (%)	96.9 (97.5)	96.9 (98.0)
Multiplicity	3.8 (3.8)	5.1 (4.9)
Rmerge (%)	31.6 (83.9)	68.6 (196.5)
Rmeas (%)	41.0 (108.5)	83.9 (242.2)
Rpim (%)	25.7 (67.8)	47.7 (139.8)
Structure Determination		
MR search models	4UTB	4UTB
NCS	2	2
Targeting	4UTA (DENV2 sE) 4UT7 (scFv A11)	4UTA (DENV2 sE) 4UT7 (scFv A11) 4LLD (CH/CL)
Use of TLS	Yes	Yes
Refinement§,‡		
Resolution	20.0-3.9 (4.1-3.9)	40.0-3.9 (4.1-3.9)
Number of Work/Test reflections	19 112/947	19 323/945
Rwork (%) / Rfree (%)	28.6/30.0 (27.3/30.9)	31.0/34.7 (37.3/37.6)
Rms deviation from ideal		
Bond lengths (Å)	0.007	0.005
Bond angles (°)	1.13	1.20
Ramachandran plot‖		
Favoured (%)	95.45	95.9
Allowed (%)	4.22	3.92
Outliers (%)	0.33	0.18

DENV2 sE: strain FGA02 (GenBank accession number KM087965.1).
The protein buffer used for all the crystallization experiments was: 150mM NaCl and 15mM Tris pH 8.
*Protein concentration was estimated using theoretical extinction coefficients of the complexes (DENV2 sE + Fab), OD280nm of the protein solution was measured before crystallization.
The theoretical extinction coefficients for individual component are: DENV2 sE-strep: 1.03; EDE2 A11 Fab: 1.68.
Extinction coefficients were calculated without taking into account carbohydrate moieties.
Hanging drop method was used for crystallization of the proteins at 18°C. One crystal was used for each of the data sets.
‡Highest resolution shell is shown in parenthesis.
§low-resolution for refinement of DENV2 sE A259C - EDE2 A11 Fab complex was truncated to 20 Å.
‖Ramachandran statistics were calculated with Molprobity.
MPD, 2-Methyl-2,4-pentanediol; PEG, Polyethylene glycol; PDB, Protein Data Bank; $CC_{1/2}$, correlation coefficient; I/σ(I), empirical signal-to-noise ratio; MR: molecular replacement; NCS: non-crystallographic symmetry; Rmeas, multiplicity-corrected R; Rpim, expected precision; TLS: parameterization describing translation, libration and screw-rotation to model anisotropic displacements.